Robust Analysis and Restoration of Noisy Images and Video

D. ABOUTAJDINE (IEEE Senior Member)
GSC-LEESA B. P. 1014
FACULTE DES SCIENCES
Rabat, MOROCCO 10000
aboutaj@fsr.ac.ma

Abstract

An important area in visual communications is that of restoring still image or image sequences distort by their transmission through a degrading channel, their acquisition, recording or storage. In this paper, we will present new algorithms developed in our group for robust analysis and restoration of still images or image sequences. The overview includes robust motion estimation, robust map disparity estimation for stereo images and restoration of images or sequences degraded by the transmission channel. Usually linear filters and second order statistics (S.O.S.) are used to extract information that is exploited to estimate parameters such as motion, disparity or channel response. Other approaches use linear or nonlinear image analysis tools to restore the degraded image. The obtained results are not always satisfactory. Some of them processes each image separately and the obtained sequence suffers from the presence of artifacts. In this paper, the concerned applications and the associated analysis tools will be recalled. Then, new approaches will be exposed and evaluated against the classical ones through a set of experiences that will show the robustness of our methods compared to the existing ones. These algorithms use the higher order statistics as information criterion. That means that we are free from the gaussianity hypothesis for the signals.

1 Introduction

Habitually, when analyzing images or image sequences, the used model doesn't include explicitly the disturbing noise whose origin can be from acquisition, recording, storage or error transmission. The processed images are supposed noise free or preprocessed. In fact these images are generally filtered using different kind of filters in general nonlinear such as median, gaussian, ... filters. The obtained results aren't satisfactory in the edges neighborhood and produce artifacts if the images are treated separately. The visual obtained quality is poor because only moving objects change from image to image and the applied filtering leads to different results for each image.

Different applications are concerned in the following. First, we will deal with the disparity map estimation in the stereovision problem. The disparity is a relative displacement of each pixel in-between the right and left images. We will show that, in the presence of noise, the correlation methods aren't efficient and the introduction of higher order correlation improves the matching results. We will also give some comparison results between the correlation, Higher Order Statistics (H.O.S.) and dynamic programming method.

The second application is the motion estimation method for coding. The estimated parameter is a displacement but, to have a compact information, we usually introduce a model for each moving object. We will use the simplified linear model with 4 parameters: (The horizontal and vertical displacements of the object center, the rotation angle and the convergence or zoom). We will report new results showing that if we include this scheme in a DCT based sequence coding method, the SNR is improved with about $3db$ for the same bit rate.

The third application is the spatio-temporeal filtering of noisy image sequences. This application uses the precedent results. First we estimate the motion model parameters then we compensate it and we apply the spatio-temporal filter which consists in a 3-Dimentional LMS L-filter. In a precedent work the authors use SOS motion estimation algorithm and a wiener filter which is efficient only in the case of uncorrelated white noise [26].

The paper is organized as follows: after the introduction, the second paragraph is dedicated to the disparity estimation using the HOS statistics. The next one presents the motion estimation algorithm and the forth is concerned with the spatio-temporal filtering of the image sequences to eliminate the noise after estimating and compensating the motion. Then a conclusion and some perspectives are given.

2 Disparity Estimation in Noisy Stereovision

Stereovision is a useful tool for obtaining depth information. It consists in finding the correspondence points between the left and right images, so that, given the camera model, the depth can be computed by triangulation. If a pair of stereo images is rectified so that the epipolar lines are horizontal, a pair of corresponding points in the right and left images should be searched for only within these lines [4, 10, 11]. This search can be treated as the problem of finding a matching path on a 2-dimensional (2D) search plane whose vertical and horizontal axes are the right and the left lines. A dynamic programming technique can handle this search efficiently [3].

In order to improve this method, we have developed a matching algorithm constrained by interest points [8]. But this technique does not consider noise effect. There are many situations where the images might be corrupted by noise. In this case, Second-Order Statistics (SOS) based methods (like dynamic programming [8, 3] or block matching [16] ...) do not work well. On the opposite, Higher Order Statistics (HOS) based methods are more advantageous since they are not affected by noises with symmetric probability density function [1, 2]. We have proposed a novel correlation method based on a Cumulant-matching criterion [7] in addition to the new constrained dynamic programming based on a Cumulant-matching criterion.

2.1 Problem Statement

Using the noiseless model defined in [1] and [2], we propose the following which take in account the noise:

$$IB_g(X) = I_g(X) + N_g(X) \tag{1}$$

$$IB_d(X) = I_d(X) + N_d(X) = I_g(X - d(X)) + N_d(X) \tag{2}$$

Where $IB_g(X)$ and $IB_d(X)$ are noisy left picture and right picture, respectively, $I_g(X)$, $I_d(X)$ are left and right noiseless ones. $N_g(X)$ and $N_d(X)$ are assumed to be zero mean with symmetric distribution noise (SDN). In addition, $d(X)$ is the disparity vector, where $X = (x, y)$ so $X - d(X) = (x - dx(x, y), y - dy(x, y))$. In this paper we are interested to rectified pictures so $dy(x, y) = 0$ [6].

Because Cumulants of this noise are theoretically zero [1, 2], estimation techniques based on these statistics suppress its effect even if it is spatially and temporally correlated.

If $C_{IB_gIB_gIB_g}$ and $C_{IB_gIB_dIB_g}$ denote third order auto-Cumulant of IB_g and Cross-Cumulant of images IB_g and IB_d

$$C_{IB_gIB_gIB_g}(m, n) = E\left[IB_g(X)IB_g(X + m)IB_g(X + n)\right] \tag{3}$$

$$C_{IB_gIB_dIB_g}(m, n) = E\left[IB_g(X)IB_d(X + m)IB_g(X + n)\right] \tag{4}$$

It is well know that the a third order Cumulant of a zero mean SDN is zero [1], thus, for coloured SDN noise, the third order Cumulant of noisy image IB(X) is equal to the third order Cumulant of the noiseless I(X) image.

In these conditions and to get a relevant map disparity estimation, we propose a new matching technique based dynamic programming by minimizing the following criterion:

$$\hat{J}_{3abs}(d) = \sum_m \sum_n \mid \hat{C}_{IB_gIB_gIB_g}(m - d, n) - \hat{C}_{IB_gIB_dIB_g}(m, n) \mid \tag{5}$$

2.2 Proposed Disparity Estimation Methods

In this paragraph, we will describe 3 methods, HOS-based correlation method, dynamic programming method and HOS-based dynamic programming method.

2.2.1 HOS-based Correlation Method

*** Method Description**

In this method, a point to be matched becomes the center of a small widow of pixels which is compared to similarity sized regions in the other image. Matching metrics are used to provide a numerical measure of the similarity between a template window in the first image and a candidate window in the second image and hence are used to determine the optimal match. A simple approach used in correlation method is to compute the value of the matching metric using a fixed window in the first image and a sliding window in the second image. The sliding window is moved in integer increments along the epipolar line, where the amount of shift is the test disparity. The disparity having the optimal value for the matching metric is then selected.

*** HOS-based Correlation Criterion**

In the previous methods, the cost function was based on a Second Order Statistics (SOS) criterion.

The cost associated with the matching of pixels (x, y) and $(x + dx, y + dy)$ is given by:

$$SAD(d) = \sum_{i=1}^{N_w} \sum_{j=1}^{M_w} | IB_g(x+i, y+j) - IB_d(x+d_x+i, y+d_y+j) | \quad (6)$$

where $NwxMw$ is the correlation window. In order to take into account the presence of noise, we have introduced the cost function based on Higher Order Statistics (SOS) given by (5).

2.2.2 Proposed Dynamic Programming Method

*** Dynamic Programming (DP)**

We use dynamic programming to solve the problem of disparity estimation. This technique is particularly adapted to optimization problems subject to constraints. The dynamic programming uses the local associations of features to condition the global optimization research. The principal idea of this technique is to minimize a cost function in a bidimensional graph.

Indeed, the problem of obtaining correspondences between right and left epipolar lines can be solved as a path finding problem on a 2D plane. For that, we have arranged the signals on the left and the right epipolar lines in two-array axis (see figure 1).

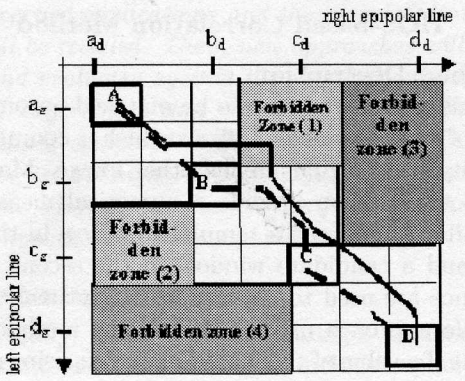

Figure 1: Dynamic programming constrained by interest points.

Order constraints and disparity domain enable the reduction of possible paths and allow the intra-line consistency [4, 3]. The advantage of this technique is that it allows the subdivision of the matching problem into a set of under-problems.

*** Constrained Dynamic Programming (CDP)**

In order to achieve inter-line consistency we have used interest-points to further constrain the possible paths [8]. After extracting and matching interest point [5, 9] they are used to define forbidden zone in the search plane: The path is constrained to contain points B and C representing the couples of homologous interest points (bd, bg) and (cd, cg). Assuming that the order constraint is verified, the correspondents of points between cd and dd are located between points cg and dg (and vice versa). This scheme defines two forbidden zones. Zone 3 permits to avoid the matching of the points of]cd,dd[interval with the $]ag, cg[$ points . Zone 4 permits to avoid matching the points of]cg,dg[interval with the $]ad, cd[$ points. Therefore, any horizontal, vertical or diagonal displacement that can browse a forbidden zone is excluded. This restriction permits a best constrained matching of epipolar lines with a reduced execution time.

*** HOS-Based Dynamic Programming**

As we did for the HOS correlation method, the criterion (6) is replaced by the (5) to take into account the noise effect.

2.2.3 Experimental Results and Discussion

We have processed 3 couples of noisy images with a synthetic noise and we have compared the disparity field obtained with 4 different methods: SOS, HOS-based correlation methods, SOS-based constrained dynamic programming and the proposed HOS-based constrained dynamic programming. The introduction of HOS information improves the robustness of the methods.

In the presence of noise SOS-based dynamic programming produces artifacts in the disparity field which are propagated along epipolar lines. On the contrary, HOS-based dynamic programming overcomes noise presence and gives a more consistent disparity map. We show the obtained results for only a pair of images called "MUR". See figures 3, 4, 5 and 6.

We have carried out a serie of experiments in order to validate the robustness of our approach in the case of noisy images. The Curves presented in figure 2 show the percentage of error points as a function of the noise variance. It shows the superiority of the HOS based methods against the SOS based ones specially for higher noise variance.

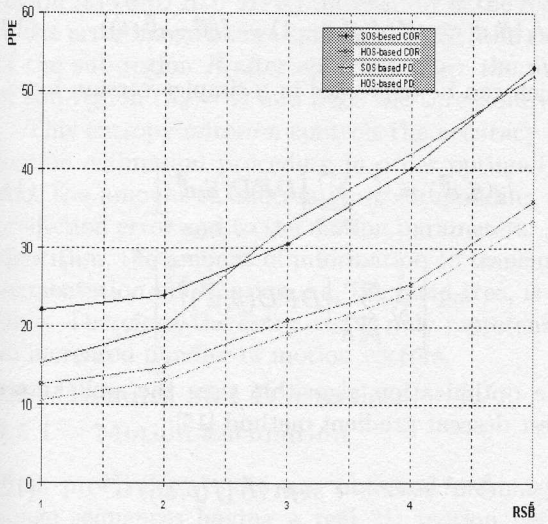

Figure 2: Influence de bruit sur les appariements erronés

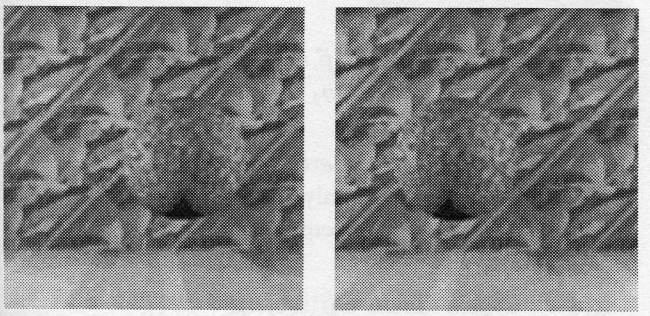

(a) (b)

Figure 3: a) Left Noisy image "MUR", b) Right noisy image "MUR"

3 Robust Motion Estimation

In many situations where video sequences are corrupted by noise, we need an efficient motion-estimation technique, which is able to track objects within noisy sources. Here, we present a technique using jointly the Higher-Order Statistics (HOS) and segmentation based regions with adaptive splitting. Experiments on synthetic and real image sequences are reported. A significant improvement of DCT coding is shown. We obtain a gain varying between 1 and $2.9dB$ for a given bite-rate.

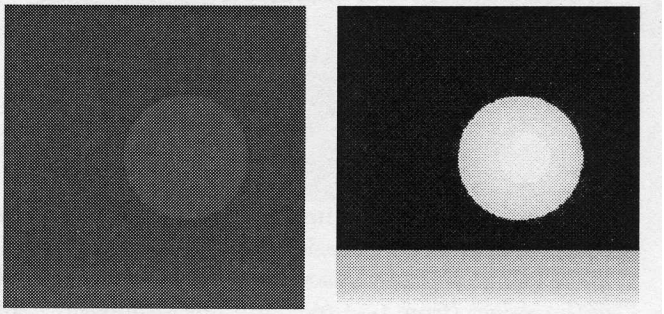

(a) (b)

Figure 4: Real disparity map a) not modified, b) modified for visualization.

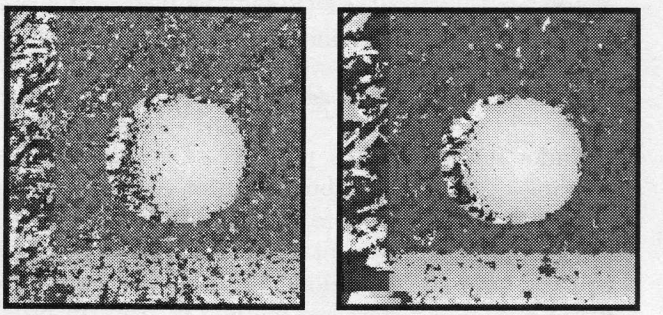

(a) (b)

Figure 5: Dense disparity map obtained by a) SOS-based correlation, b) HOS-based correlation

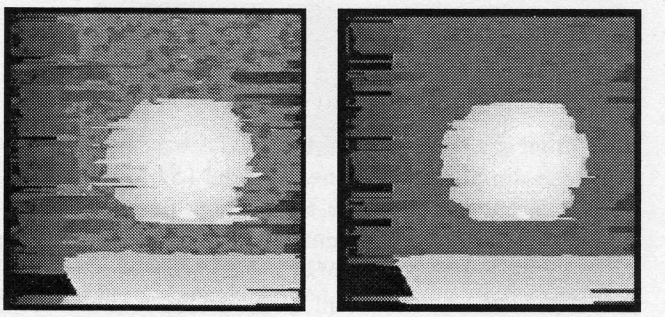

(a) (b)

Figure 6: Dense disparity map obtained by a) SOS-based dynamic programming, b) HOS-based dynamic programming.

3.1 Problem Formulation

Two consecutive noisy images are modelled as (9):

$$\begin{aligned} f(\vec{p},t) &= I(\vec{p},t)+n(\vec{p},t) \\ f(\vec{p},t+1) &= I(\vec{p},t+1)+n(\vec{p},t+1) \\ &= I(\vec{p}-\vec{d},t)+n(\vec{p},t+1) \end{aligned} \quad (7)$$

Where f is the noisy image,I the noiseless one, n a coloured zero mean Gaussian noise of unknown covariance, t time, $\vec{p}$ position, and $\vec{d}$ the displacement vector of the object (from $t-1$ to t). In this formulation, the basic assumption is intensity constancy, as follows:

$$I(\vec{p},t+1) = I(\vec{p}-\vec{d},t) \quad (8)$$

The problem is to estimate $\vec{d}$ from the observation of $f(\vec{p},1)$ and $f(\vec{p},t)$. The classical solution to obtain the displacement vector requires minimising the mean square error of the $DFD(\vec{p},\vec{d})$. The displaced frame difference (DFD) is defined [21] as follows:

$$DFD(\vec{p},\vec{d}) = f(\vec{p},t+1) - f(\vec{p}-\vec{d},t) \quad (9)$$

Unfortunately, in the presence of coloured Gaussian noise (CGN), the above solution may lead to inaccurate results. In these circumstances, HOS-based methods are more advantageous since they are blind to such noise [1, 9]. Along this way, we have proposed a HOS region-based method in [15]. In order to complete and to improve the performances of the previous technique, we introduce into the algorithm a segmentation.

3.2 Motion Estimation

In this stage we use a HOS region-based technique to estimate global motion parameters proposed in [15]. This technique includes motion modelling, initialisation, and optimisation steps.

3.2.1 The Motion Model

In order to describe the motion of every region, we choose the Simplified Linear Model (SLM) described by a vector $\theta = (t_x, t_y, k, \theta)^T$. These parameters correspond to 2D components of apparent translations (t_x, t_y), divergence ratio $(k)$and rotation angle (θ).

The merit of this form of modeling is that it provides a compact representation for the description of the field and a good characterization of the elementary $3-D$ apparent object motions [17, 18].

3.3 Optimisation

Restricting ourselves to one region, the motion vector is computed from the optimization of the kurtosis measure [1]:

$$J_4(\vec{p},\vec{d^i}) = K(f(\vec{p},t+1) - f(\vec{p}-\vec{d^i},t)) \quad (10)$$

which can be expressed in a simpler version by:

$$\hat{J}_4(\vec{p},\vec{d^i}) = \frac{1}{N}\sum_{\vec{p}\in R}\left[DFD(\vec{p},\vec{d^i})\right]^4 - 3\left[\frac{1}{N}\sum_{\vec{p}\in R}\left[DFD(\vec{p},\vec{d^i})\right]^2\right]^2 \quad (11)$$

The optimization algorithm uses the well known steepest descent gradient method [15]:

$$\hat{\Theta}^{i+1} = \hat{\Theta}^i - \epsilon\ sign\left(K[f(\vec{p},t)]\right)\vec{G}^i \quad (12)$$

where ϵ is the 4×4 diagonal matrix of gain, Sign () is the signum function, this term showed that the algorithm is based on maximizing or minimizing the mean-kurtosis error (depending on the sign of the sample kurtosis of the signal) [22] and G given by: (13)

$$\vec{G}^i = \left[\frac{\partial J_4(\vec{p},\vec{d^i})}{\partial\theta_1}\ \frac{\partial J_4(\vec{p},\vec{d^i})}{\partial\theta_2}\ \frac{\partial J_4(\vec{p},\vec{d^i})}{\partial\theta_3}\ \frac{\partial J_4(\vec{p},\vec{d^i})}{\partial\theta_4}\right] \quad (13)$$

Here, motion parameters are estimated for each region, which allow analysing and compressing efficiently complex image sequences.

3.4 Quad-Tree Splitting

The estimation of the motion models needs the choice of a segmentation procedure, either prior, or simultaneous with, the motion estimation step itself, since this operates on a region R of matched pixels. The segmentation rule influences greatly the overall performances of the algorithm. In this study, images are segmented into motion homogenous regions using an adaptive quad-tree splitting. This segmentation allows the progressive decomposition of the image into smaller and smaller regions making it possible firstly to identify the more global attributes and leading to the identification of local motions at the end of the estimation process. Clearly, a splitting criterion has to be defined. The test adopted consists in comparing the entropy of the motion compensated differences as follow:

$$N(R)H(R) - \sum_{i}^{n_d} N(R_i)H(R_i) > S_H \quad (14)$$

where $N(R)$ (resp. $N(R_i)$) : the number of pixels in region R (resp. R_i). $H(R)$:the entropy of the region R in the error image before splitting. $H(R_i)$:the entropy of the sub-region $R_i$after splitting. n_d : the number of sub-region ($n_d = 4$) and $S_H$is the threshold value.

This entropy criterion controls the accuracy of the motion estimation procedure in order optimally balance the amount of information corresponding to the prediction error and to the motion parameters. In the algorithm, the amount of information to transmit the segmentation information, i.e, the quad-tree, is negligible. Therefore, the extra cost is only represented by an increased number of motion vectors.

3.5 Results and Discussion

3.5.1 Motion Estimation

First promising results are obtained on noisy TV image sequences having a real 2D motion perfectly known (Fig. 7). They are obtained using zero-mean, spatially, and temporally correlated noise.

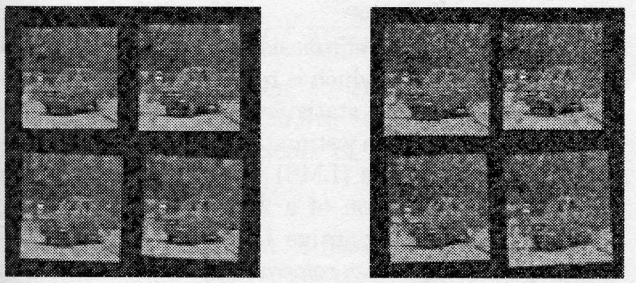

Figure 7: Noisy images with $SNR = 10dB$ at time $t(a)$ and time $t+1(b)$. Region 1 (NE): pure translation $tx = 2$, $ty = 2$, region 2 (NW): pure divergence $k = -0.1$, region 3 (SW): pure rotation $\theta = 0.07$and region 4 (SE): composed motion $k = -0.1$ and $\theta = 0.1$.

Simulations are made, using both our HOS-method and a similar SOS one [2]. The proposed method allows an accurate estimation of the motion parameters. It indicates also that it is much less sensitive to the noise as compared to SOS-based method.

3.5.2 Motion Segmentation

In this section, experimental results obtained with a real image sequence (Fig. 8) are presented. " campagne" is a complex scene with a global motion of divergence and others local motions (car, a post on the right of the picture, leaf of trees).

For the experiments, the decomposition starts from 32×32 initial regions to 8×8 final regions. For the

Figure 8: One frame of the noisy images sequence "Campagne" with SNR=10 dB.

SOS-based method the splitting threshold is based on a Mean Square Error (MSE) criterion.

The results given in figures 9 and 10 illustrate the performances achieved using the proposed method, as compared to SOS-based one, concerning the quality of motion fields, the motion compensated error and the obtained quadtree segmentation. As opposed to the SOS- method, ours gives less splitting regions which corresponds effectively to the zones of local motion (Figures 9.b and 10.b)

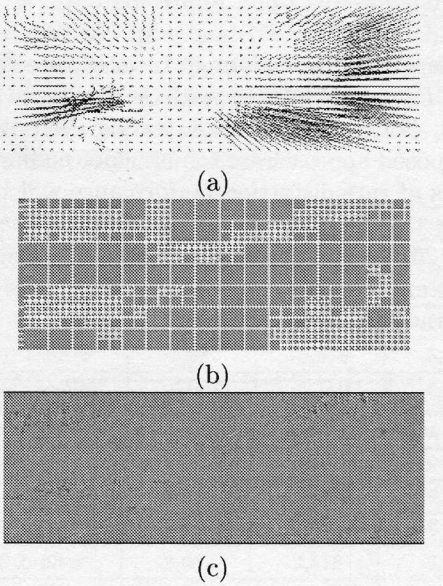

Figure 9: Motion compensation of the "Campagne" sequence using proposed method. a) Motion compensated differences($MSE = 26.5$), b) quadtree segmentation, c) Motion vector field

3.5.3 Motion Compensation Coding

In this section, we examine the proposed algorithm with respect to its application to robust video coding

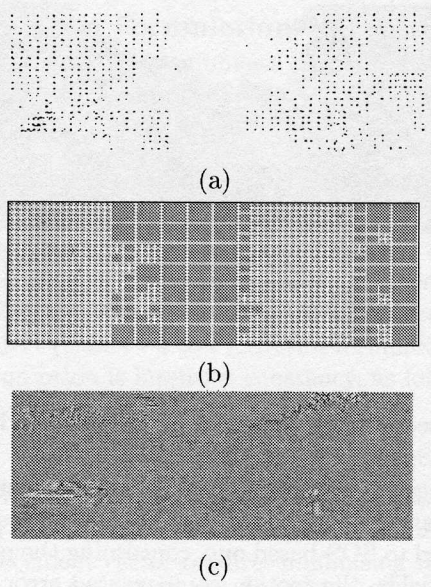

Figure 10: Motion compensation of the "Campagne" sequence using SOS method. a) Motion compensated differences (MSE=98.6), b) quadtree segmentation, c) motion vectors field.

and compare its behaviour in term of rate-distortion for DCT coding scheme with a similar SOS-based method. Some results demonstrating the potential of the proposed approach for robust video coding scheme in terms of rate-distortion performance will be given. Varying the DCT quantization step over values 40, 35, 30, 25, 20 and 15 generates rate-distortion plots. In these experiments, we use the DCT tables given in $H263$ standard [20].

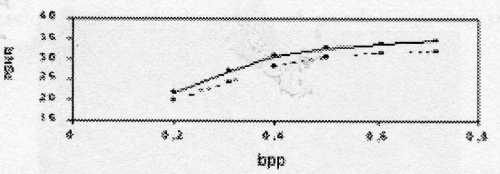

Figure 11: $PSNR$ (average) Vs the bit-rate for the sequence ' campagne' for both methods ; SOS-method: dashed HOS-method: solid.

Figure 11 shows the average PSNR over 10 frames from reconstructed frames produced by HOS-method, and SOS-method function of the bit-rate. From this rate-distortion curves with HOS-method (solid line) and SOS-method (dashed line), it can be seen that the proposed method has higher rate-distortion performance for this sequence, which improves the quality of coding. Significant gains in PSNR between 1 and $2.9dB$ are achieved for the sequence tested over SOS-based method.

4 An Efficient Spatiotemporal Filter for Noise Reduction in Video Sequences

This part deals with denoising video sequences using a motion compensated spatiotemporal filter. Motion compensation is performed by the robust estimator discribed in the precedent paragraph. Then, a 3-D LMS L-filter is applied. The experimental data prove that the proposed solution results in improved efficiency of video restoration.

4.1 Problem Statement

To reduce noise in image sequences several temporal and spatiotemporal filtering schemes have been proposed [25].

In general, spatiotemporal filter performance will be improved with accurate motion estimation and compensation [24].

In this paper, the emphasis is on the development of a filtering scheme which is robust to motion estimation errors and noise statistics. It uses a parametric motion compensation estimator and a spatiotemporal least mean square (LMS) L-filter. The 3-D LMS L-filter is an extension of a 2-D LMS L-filter. The superiority of 2-D adaptive L-filters over the adaptive linear filter in noise removal applications has been demonstrated [23]. The motion estimator is a region recursive higher order statistics (HOS) based method which uses a simplified affine motion model well suited to the analysis of complex noisy image sequences as shown in the precedent paragraph.

4.2 Noise Filtering

The noisy sequence is modeled as follows $g_n(i,j) = f_n(i,j) + \eta_n(i,j)$. Where $g_n(i,j)$ denotes the intensity of the pixel (i,j) of the n^{th} frame of the observed sequence, $f_n(i,j)$ stands for the intensity of the pixel (i,j) of the n_{th} frame of the original sequence and $\eta_n(i,j)$ denotes the additive Gaussian noise. The adaptive LMS L-filter's output is defined by the linear combination of the order statistics of the input samples in the filter window. The intensity estimate at image location (i,j) for the n_{th} image is computed using a cube of size $(2p+1) \times (2q+1) \times (2l+1)$ and is given by

$$\hat{f}_n(i,j) = \sum_{(p,q,l) \in S} \hat{a}(p,q,l) g^r_{n-l}(i-p, j-q) \quad (15)$$

where S is the filter support, $g_n^r(i,j)$ is the ordered observations and $\hat{a}$ is the LMS recursive L-filter coefficients vector that minimizes the mean square error between the estimated and the original images given by :

$$\hat{a}(s+1) = \hat{a}(s) + \mu\epsilon(s)g_n^r(s) \qquad (16)$$

where $s = (i,j)$ denotes the pixel location, $\epsilon(s)$ is the estimation error at pixel s, i.e., $\epsilon(s) = \hat{f}(s) - f(s)$ μ is the step-size parameter.
In theory, sufficient conditions on μ exist that guarantee the convergence of the LMS algorithm. These conditions depend on the knowledge of the eigenvalues of the correlation Matrix. When the adaptive filter is to operate in nonstationnarity environment, it is reasonable to employ a time/space varying step-size parameter $\mu(s)$. If $\mu(s)$ is choosen to be:

$$\mu(s) = \frac{1}{\|g_n^r(s)\|^2} \qquad (17)$$

then coefficient vector will be modified as follow :

$$\hat{a}(s+1) = \hat{a}(s) + \frac{\mu_0}{\|g_n^r(s)\|^2}\epsilon(s)g_n^r(s) \qquad (18)$$

μ_0 should be chosen to satisfy the inequality $0 < \mu_0 \leq \frac{2}{3}$. This recursive equation describes the adaption of the coefficients of the normalized LMS L-filter (NLMS L-filter).

The signal-dependent L-filter (SDNLMS L-filter) structure allows to separate treatement of the edges and the homogeneous image region. It consists of two NLMS adaptive L-filters whose outputs $\hat{f}_L(s)$ and $\hat{f}_H(s)$ (Low and High-frequency data, respectively) are combined to give the final reponse as follows:

$$\hat{f}(s) = \hat{f}_L(s) + \beta(s)\{\hat{f}_H(s) - \hat{f}_L(s)\}. \qquad (19)$$

The local signal-to-noise ratio measure is given by $\beta(s) = 1 - \frac{\sigma_\eta^2}{\sigma_g^2(s)}$, where σ_η^2 is the global noise variance and $\sigma_g^2(s)$ is the local variance of the noisy input observations. The adaptive L-filters may use different window sizes. In such a case, the coefficient $\beta(s)$ can be used as a signal-dependent switch between the two NLMS adaptive L-filters, i.e., $\hat{f}(s) = \hat{f}_H(s)$ if $\beta(s) > \beta_t$, otherwise $\hat{f}(s) = \hat{f}_L(s)$, where $0 < \beta_t < 1$ is a threshold that determines a trade-off between noise suppression and edge preservation.

4.3 Experimental Results

We used some frames which are part of Trevor White sequence which involve moving objects in the foreground. We show in Figure 12 the comparison between the LMS L-filters in suppressing mixed impulsive and additive white Gaussian noise in the 3rd frame of Trevor White sequence. The output of the 3-D median filters is given as a reference. The motion compensated original image corrupted by mixed impulsive and additive white Gaussian noise is shown in Figure 12.b. The filtered image using the linear NLMS filter and the output of the NLMS L-filter are shown in Figure 12.c and 12.d, respectively. The ouput of the SDNLMS L-filter structure that employs two NLMS L-filters of dimensions 5×5 and 3×3 to smooth the image data in homogeneous regions and close to the edges, respectively, is shown in Figure 12.e . The visual evaluation demonstrates the superiority of the SDNLMS L-filter in preserving the texture found in the background of the image.

The filtered images quality is also evaluated by measuring the Signal-to-Noise Ratio improvements. Table 1 summarizes the SNR improvements achieved by various L-filters in smoothing, respectively some frames of Trevor White sequence with mixed impulsive ($p = 5\%$) and additive white Gaussian noise ($\sigma = 20$) and the same sequence with additive white Gaussian noise ($\sigma = 20$). For white additive Gaussian noise, both linear NLMS filter and NLMS L-filter have the same improvement and the signal-dependent is lightly better. For mixed impulsive and additive white Gaussian noise, we observe that the best results are obtained by the SDNLMS L-filter.

Noise Type	Gaussian Noise		
Method	3th frame	5th frame	7th frame
Median 3×3	-5,232	-5,367	-5,272
linear NLMS filter	-5,849	-5,200	-5,900
NLMS L-filter	-5,632	-5,878	-5,433
SDNLMS L-filter	-6,097	-6,140	-6,149
Noise Type	Mixed impulsive and Gaussian Noise		
Method	3th frame	5th frame	7th frame
Median 3×3	-8,780	-8,469	-9,330
linear NLMS filter	-8,619	-8,082	-8,575
NLMS L-filter	-9,632	-9,578	-9,611
SDNLMS L-filter	-10,257	-10,460	-10,634

Table 1: SNRi in (dB) achieved by various L-filters in smoothing some frames of Trevor White sequence that has been corrupted additive white Gaussian noise ($\sigma = 20$) and the mixed impulsive (5%) + additive Gaussian noise ($\sigma = 20$)

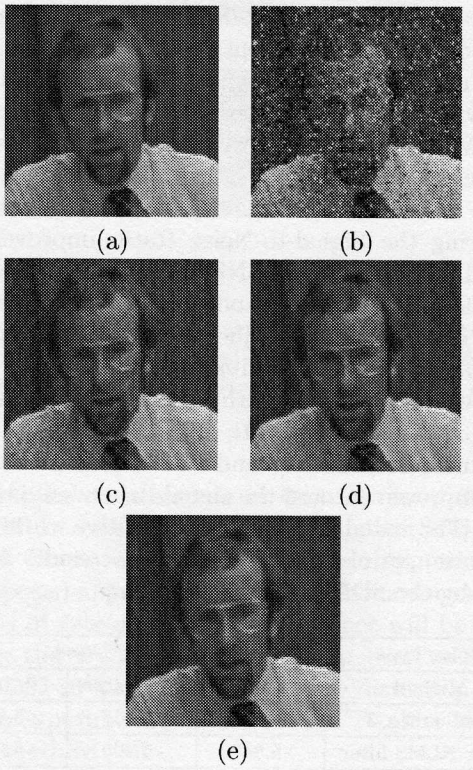

Figure 12: (a) Original Trevor 3th frame 256 × 256, (b) Compensated motion image corrupted by mixed impulsive ($p = 5\%$) and Gaussian additive noise ($\sigma = 20$), (c) Output of the 3×3 linear NLMS filter with ($\mu_0 = 0.8$), (d) Output of the 3×3 NLMS L-filter with ($\mu_0 = 0.8$), (e) Output of the SDNLMS L-filter that employs two NLMS L-filters of dimension 5×5 and 3×3 with ($\mu_0 = 0.8$) and ($\beta_t = 0.7$).

5 Conclusion

Altogether, the proposed work demonstrates the utility of our approaches for disparity and motion estimation parameters and their use for coding and denoising in the case of noisy image sequences. Our scheme in [15] is extended by more efficient segmentation step that improves motion compensation performance. The results show that with this approach, noisy sources can be compressed robustly.

In the third approach, we presented a 3-D adaptive LMS L-filter for noise suppression in image sequences. Among the several tested versions LMS L-filter has provided a significant improvement for severely corrupted images.

Other investigation are carried out. Some of them are in progress and give promizing results. It's the case for the approches based on the Hypergraph theory that we are developping.

References

[1] Anderson J. M. and Giannakis G. B., "Image motion estimation algorithms using Cumulants," *IEEE. Trans. On Image Processing*, vol. 4, no.3, March 1995 pp 346-357.

[2] Anderson J. M. and Giannakis G. B., " Noise insensitive image motion estimation algorithms using Cumulants," *Proc. ICASSP'91*, vol. 4, Toronto, CANADA, p 2721- 2724, May 1991.

[3] Baker H. H., Binford T. O., " Depth from edge and intensity based stereo," *Proc. 7th Int. Joint Confer. On Artificial intelligence, Vancouver, Canada,* Aug. 1981.

[4] Ohta Y. and Kanade T., "Stereo by intra and inter scanline search using dynamic programming," *IEEE PAMI* 7(2) : 139-154, March 1985.

[5] Harris C. et Stephens M., "A Combined Corner and Edge Detector," *in Proc. 4th Alvey Conference,* pages 147-151, Manchester, 1988.

[6] Papadimitriou D.V., Dennis T.J., "Epipolar line estimation and rectification for stereo image pairs," *IEEE trans. On image processing* vol. 5(4), 1996.

[7] Rziza M., Ibn Elhaj E., Belbzioui N., Aboutajdine D., " Estimation de la carte de disparité pour les images bruitées," *CORESA, Poitiers,* France, Octobre 2000.

[8] Rziza M., Tamtaoui A., Morin L., Aboutajdine D., " Estimation and segmentation of a dense disparity map for 3D reconstruction," *Proc. ICASSP'00,* Istanbul, Turkey 2000.

[9] Zeller C., "Projective, affine et euclidienne en vision par ordinateur et application a la perception tridimensionnelle," *Thèse de l'école polytechnique* de Grenoble 1996.

[10] Barnard S., Fischler M., " Computation stereo," *Surv. 14 No.* pages 553-572, 1882.

[11] Ayache N. " Artificial Vision for Mobile Robots," *MIT Pres* Cambridge, MA, 1991.

[12] Banks J., Bennamoun M., Corke P., " Fast and Robust Stereo Matching Algorithm for Mining Automation," *Digital Signal Processing 9,* pages 137-148, 1999.

[13] Hannah M., " Computer Matching of Areas in Stereo Images," *Ph.D. thesis,* Stanford university, 1974.

[14] E. Ibn Elhaj, D. Aboutajdine, S. Pateux, L. Morin. " Méthode région-récursive d'estimation de mouvement des séquences d'images bruitées." *17ème colloque GRETSI,* Vannes 13-17 septembre, 1999.

[15] E. Ibn Elhaj, D. Aboutajdine, S. Pateux, L. Morin. " HOS-based method of global motion estimation for noisy images sequences" *IEE Electronics Letters,* 1999.

[16] G. Tziritas, C. Labit, " Motion Analysis for Image Sequence Coding," *in Advances in Image Communication,* vol. 4 New York : Elsevier, 1994.

[17] G. Adiv, " Determining three dimensional motion and structure from optical flow generated by several moving objects " *IEEE PAMI,* July 1985, Vol. 7, no.4.

[18] H. Nicolas, C. Labit, " Global motion identification for image analysis and coding " *Proc. ICASSP 91,* Toronto, Canada, vol. 4, p 2825-2828,.

[19] E. Sayrol, A. Gasul and J. R. Fonollosa, " Motion estimation using Higher Order Statistics," *IEEE Trans., On image processing,* vol. 5,n^o 6, june 1996, p. 1077-1084.

[20] ITU-T, " Recomendation H.263," *video coding for low bitrate communication.*

[21] A. N. Netravali and J. D. Robbins, " Motion-compensated television : Part I " *Bell Syst. Tech. J.* vol. 58, Mars 1979, p. 613-670.

[22] J. K. Tugnait, " Time delay estimation in unknown spatially correlated Gaussian noise using higher-order statistics " *In Proc. 23 rd Asilomar Conf. Signals, Syst.,Comput., Pacific Grove,* CA. 1989, p. 211-215.

[23] C. Kotropoulos, I. Pitas, " Adaptive LMS L-Filters for Noise Suppression in Images " *IEEE Trans. On Image Processing,* vol. 5, no. 12, pp. 1596-1609, December 1996.

[24] K.J. Boo and N.K. Bose, " A motion-compensated spatio-temporal filter for image sequences with signal dependent noise " *IEEE Trans. Cir, and Syst. for Vid. Tech.* vol. 8, no. 3, pp. 287-298, June. 1998.

[25] S.A. C. Kokaram. " Motion Picture Restoration: Digital Algorithms for Artefact Suppression in Degraded Motion Picture Film and Video " *Springer Verlag, ISBN* 3-540-76040-7, 1998.

[26] F. Dekeyser, P. Perez and P. Bouthemy. " Restoration of noisy, blurred, undersampled image sequences using parametric motion model" *Réseaux et Systèmes Répartis, Calculateurs Paralleles, Numero special Image et Vidéo.* Vol 12 n^o 3-4, 2000.

Acknowledgements

This work has been supported by the project 'Pars_CNR n^o 36'